An Improved IEEE 802.11 CSMA/CA Medium Access Mechanism Through the Introduction of Random Short Delays

Nirmala Shenoy, John Hamilton, Andres Kwasinski and Kaiqi Xiong
Rochester Institute of Technology, Rochester, NY 14623
Email: {nxsvks,jfhsms,axkeec,kxxics}@rit.edu

***Abstract*—The work in this paper studies the performance of Carrier Sense Multiple Access/Collision Avoidance (CSMA/CA) medium access control (MAC) mechanism in IEEE 802.11 DCF. From studying the propagation delay and clock synchronization differences between terminals, it is concluded that the slight timing differences, effectively a relative jitter, contributes to reducing the probability of collisions after a MAC backoff. This lesson is leveraged in a presented new CSMA/CA MAC technique that deliberately introduces a random short delay, akin to jitter, in the backoff slots time structure. The new medium access technique is evaluated through both an analytical model and simulations that consider the realistic timing constraints set in the IEEE 802.11 standard. Simulation results show improvements in normalized saturated throughput with the new technique from at least 14% for 10 nodes up to 26% for 50 nodes.**

I. Introduction

The analysis and design of wireless ad-hoc networks is particularly challenging because of their decentralized and self-coordinated nature. To efficiently harness wireless ad hoc networks it is important to understand the effects of the multiple factors that affect performance. Among the different components of a wireless ad-hoc network, a medium access control mechanism is one of the most challenging to design because of the need for operation in a distributed fashion. The IEEE 802.11 Distributed Coordination Function (DCF) protocol is a frequent choice for the function of medium access control (MAC) because it meets the needed requirements. As expected, the popularity of the IEEE 802.11 DCF protocol has significantly increased the study of its performance in terms of throughput and access delay.

A majority of the works concerning with the performance of the IEEE 802.11 DCF medium access control protocol have assumed node saturated conditions where all nodes have a packet to transmit all the time. This is an assumption that is convenient to investigate medium access contention and latency without being encumbered by the packet waiting time in a node's queue. The saturated conditions assumption has been extended, then, to a more realistic environment under unsaturated conditions. Under the unsaturated conditions, studies are directed towards both one-hop networks and multi-hop networks. Multi-hop networks are impacted by hidden terminals and hence perform differently than one-hop networks. Analytical models based on Markov chains, queuing theory and information theory have been proposed and their results have been very often validated with simulations. The work in [1] is widely considered to be the seminal work in analytically modeling the IEEE 802.11 DCF protocol. This work is based on the use of a Markov chain to model the status of the backoff window and the assumption that each transmission attempt is associated with a constant probability of collision regardless of the number of successive retransmissions experienced by the transmitting node. This work was followed by [2] and [3], which considered the maximum number of allowed retransmission attempts, by [4], which modified the Markov chain model in [1] to consider the status of the previous time slot effect on the transmission probability, and by [5] and [6], which introduced in the analysis a probability for backoff counter freezing. Most recently, [7] refined the calculation for the probability of backoff counter freezing by introducing a Markov chain to describe the channel states (either "Successful", "Collision" or "Idle") when a node is backing off.

All the works cited so far focus on the study of the MAC layer and, in doing so, do not include considerations of the impact from detailed practical phenomena at the physical layer. In this paper we first study the effects on the IEEE 802.11 DCF performance of the different propagation delays and clock synchronization between nodes. The study presented herein will show that the slightly different propagation delays between nodes has a positive performance impact on the MAC layer and that strict clock synchronization has a negative performance impact. To the best of our knowledge, no other research work has investigated the major impacts on IEEE 802.11 DCF of these two factors. In other works, all models have assumed that the clocks are synchronized and that the propagation delays are equal for all nodes and will not impact transmissions or collisions. A few published studies have investigated the impact of model assumptions for the IEEE 802.11 DCF mode of operation. Specifically in [8], the authors focus on the assumption that transmissions occur in discrete times clocked by the slot time, where slot times may not be accurate due to drift in local clocks at the nodes. This study was conducted using eighteen wireless devices. In [9] the same authors state that in the models studied up to that time assumptions related to the station buffer may not had been accurate. This study was also limited by the number of wireless devices in an experimental environment. Though [8] and [9]

978-3-9018-8273-9/15/

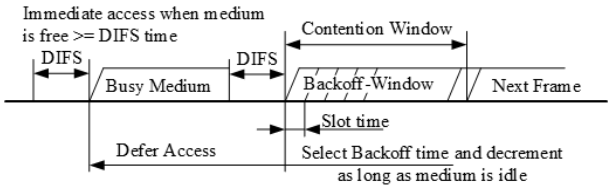

Fig. 1. The 802.11 DCF medium access control (based on [10]).

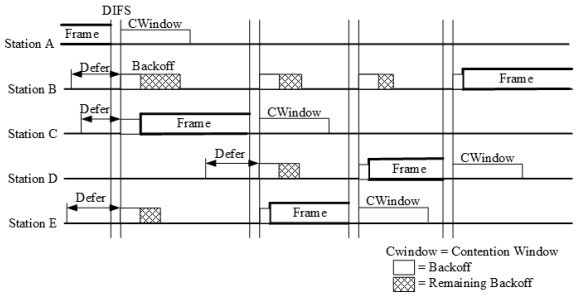

Fig. 2. The 802.11 DCF medium access control - multiple nodes (based on [10]).

studied the possible impacts of assumptions made in earlier models, their significant positive impact on the performance with increasing number of nodes was not revealed. Our study exposes the effects of clock synchronization and propagation delay differences. In fact, it will be seen that the performance improvement seen with unsynchronized clocks grows with increasing number of nodes. As this study is directed to the performance of the MAC layer, to stress the role of the medium access protocol, we focus on a saturated network where all nodes are one-hop from one another. Importantly, the lessons learned from studying the effects of different propagation delay and strict clock synchronization are used to reveal changes that could improve the performance of the IEEE 802.11 DCF protocol. As such, we introduce a new CSMA/CA medium access technique that deliberately introduces a random short delay, akin to jitter, in the backoff slots time structure. The simulation results to be presented show improvements in normalized saturated throughput with the new technique from at least 14% for 10 nodes up to 26% for 50 nodes. The simulation results were validated with an analytical model also developed in this paper.

The rest of this paper is organized as follows. First, we provide in Section II a brief summary of the IEEE 802.11 DCF protocol, followed by the description of the detailed OPNET simulation model in Section III. Section III also presents the study of the impact on performance of propagation delay and clock synchronization. Section IV presents the novel CSMA/CA medium access technique and its analytical model is studied in Section V. Concluding remarks are given in Section VI.

II. System Setup and Background

We consider a single-hop ad-hoc network where medium access control is implemented using the IEEE 802.11 DCF protocol. The network consists of n nodes with the transmit queue assumed in a saturated condition, i.e. there is always a packet waiting to be transmitted at all nodes. In the analysis, it is assumed that packet errors on the channel occur only due to multiple access collisions. From a problem setup perspective all nodes are identical. Therefore, when needed for analysis purposes, a single generic node, called the *"Tagged Node"*, is singled out to study the events it experiences.

Figure 1, based on the standards [10], describes the general 802.11 DCF access mechanism. The DCF operation uses the time intervals of SIFS and DIFS to differentiate and prioritize between ongoing sessions, comprising of DATA-ACK or RTS-CTS-DATA-ACK message sequences, and the operations of a node that has yet to gain access to the medium. While the medium is busy, all nodes that are not sending defer transmission for the duration of the busy time plus one DIFS time. At the end of this time, the nodes enter into the contention mode by randomly choosing a count-down number from a range of possible values determined by a back-off window. The back-off window size is determined by the number of successive retries to access the medium by a node. During back-off, the nodes count to zero from the number chosen at random, with each decrement of the count having a period equal to one slot time. An important concept in this paper is the "slot time," hereafter defined as the period of time elapsed between two successive decrements of the back-off counter. Importantly, this definition implies that the duration of the slot time is not fixed, as there exists events (mainly that the medium stops being idle) that may stop the counting of the back-off counter. The case when there are multiple contending nodes follows the same principles and is illustrated in Figure 2, based on the standards [10].

As discussed earlier, the first work studying the performance of IEEE 802.11 DCF is [1]. We now present a summary of this study with the focus on introducing formulation and concepts of key importance in the sequel. Further details can be found, of course, in [1]. The study in [1] was based on modeling the different medium access states into a Markov chain from where several variables affecting performance are derived. The Markov chain models the evolution of two interrelated stochastic processes: $s(t)$, which represents the back-off stage at time t, and $b(t)$, which represents the value of the back-off counter at time t. To proceed in the study, it is assumed that the back-off contention window doubles in size after each unsuccessful transition attempt, following the rule

$$W_j = \begin{cases} 2^j W_{min}, & \text{if } 0 \le j < m \\ 2^m W_{min}, & \text{if } m \le j < L, \end{cases}$$

where W_j is the contention window size at back-off stage j, W_{min} is the minimum contention window size, m is the maximum number of successive times that the contention window size can be doubled following an unsuccessful transmission attempt (that is, the maximum window size is $W_{max} = 2^m W_{min}$), and L is the maximum number of

successive retransmission attempts. Next, a key variable that is determined from the Markov chain is the probability τ that a node transmits in a randomly chosen slot time. This is equivalent to the stationary probability that the value of the back-off counter equals zero in all back-off stages. From [1],

$$\tau = \frac{2}{1 + W_{min} + pW_{min}\left[\frac{1-(2p)^m}{1-2p}\right]}, \quad (1)$$

where p is the probability that a packet will collide during a transmission attempt. The probability p can also be thought as the probability that in a time slot, one or more of the $n-1$ remaining nodes also transmit a packet. Then, p can also be written as

$$p = 1 - (1-\tau)^{n-1}. \quad (2)$$

Note that (1) and (2) form a system of two equations that can be used to calculate the value of p and τ given the parameters that define the evolution of the contention window size. Also, note that the derivation of (1) assumes that the retry limit L is infinity. If the retry limit is finite, it is possible to show that this equation becomes

$$\tau = \frac{2\left(1-p^{L+1}\right)}{1 + W_{min} + pW_{min}\left[\frac{1-(2p)^m}{1-2p}\right] - p^{L+1}\left(1 + W_{min}2^m\right)}.$$

A point of interest related to the model in [1] is some recent confusion on whether the model includes the event of freezing the back-off counter when sensing the carrier. While some works assert that this event was not included, [7], this effect is accounted for in [1] within the framework of what was called "frozen time". In fact, it is stated in [1] that "*the back-off decrement is stopped when the channel is sensed busy, and thus the time interval between two consecutive time slot beginnings may be much longer than the slot time size, as it may include a packet transmission*", which implies that a slot time should include any frozen time, such as a packet transmission, that may occur before the next back-off time counter decrement. Consequently, we based this work on the model in [1]. The only limitation in this model is that it assumes that the retry limit L is infinity. As will be seen later, this work will consider both L equal to infinity and equal to a finite number that is chosen as $L = 3$.

III. Performance Impact of Propagation Delay and Strict Clock Synchronization

We study the effect of slight propagation delay differences between nodes and strict clock synchronization on the IEEE 802.11 DCF performance through a detailed OPNET simulation. The OPNET model developed by us was validated against several operational scenarios from [1], namely, the CSMA/CA basic access with minimum contention window, W_{min} of 32 and 128 with an m value of 3 and 5 and also RTS-CTS based medium access with minimum contention window of 32 and 128 with $m = 3$. To reproduce and compare with the results in [1] (and other derived works), we set the data transmit rate at 1 Mbps. Importantly for the present study, we used the OPNET wireless transmission modules allowing for proper and accurate modeling of propagation and transmission delays. In the IEEE 802.11 DCF standard, the slot time is defined with a duration of 50μs, for the Frequency Hopping Spread Spectrum physical (PHY) layer. A receiver operating with these specifications is able to detect a conforming signal with a specified synchronous detection pattern up to 22μs after the start of the slot time. If the start of a transmission is asynchronous and the signal arrives after the start of the slot but at least 16μs prior to the end of the slot, the PHY layer shall indicate a busy channel prior to the end of the slot time with asynchronous detection. Following the standard, the slot time duration included in the simulation a receive-to-transmit turnaround time and the energy detect time. Also as dictated in the standard, the propagation delay is regarded as being included in the energy detect time. For Direct-Sequence Spread Spectrum (DSSS) as PHY layer, the slot time is 20μs. The slot time for the Orthogonal Frequency Division Multiplexing PHY shall be 9μs for 20MHz channel spacing, shall be 13μs for 10 MHz channel spacing, and shall be 21μs for 5 MHz channel spacing. In this article we adopted the FHSS PHY system because the majority of previous related works, which we wanted to leverage, are based on this model. However, the contributions of this work are general and should apply to all PHY layers regardless.

Space limitations prevent us from presenting results from all the validation tests that were conducted. Consequently, we show only one set of validation results, obtained for a configuration with the basic access DCF mode of operation, $W_{min} = 32$ and $m = 5$. However, to highlight the impact on performance depending on whether L is infinite or a finite number, we include Figure 3 which compares simulation results for normalized saturation throughput with $L = \infty$ and with $L = 3$. To validate the simulation results, Fig. 3 also includes the saturated throughput as determined from the analysis in [1]; it can be seen how the curve corresponding to the analytical results from [1] (labeled "Bianchi Analytical") shows a close match with the results from the OPNET simulation with $L = \infty$. When the number of retries is made limited, the throughput is reduced because after L retries the packet is dropped and a new packet with a minimum contention window contends for the medium. This leads to more collisions. When L is infinity, the packet is never dropped and will repeatedly contend for access to the medium with the maximum contention window and hence reducing the collision probability and improving the normalized saturation throughput. Because of the close match between the OPNET simulation and the analytical results from [1], the validation test also verifies the implicit assumption of frozen counters in the models from [1] and its accuracy.

We applied the OPNET simulation tool to the study of the effect of slight differences in propagation delay on the IEEE 802.11 DCF protocol performance. The OPNET simulation tool implements realistic transmitter and receivers models that incorporate propagation delays based on distances between nodes, transmission delays, antenna power gains, and noise in

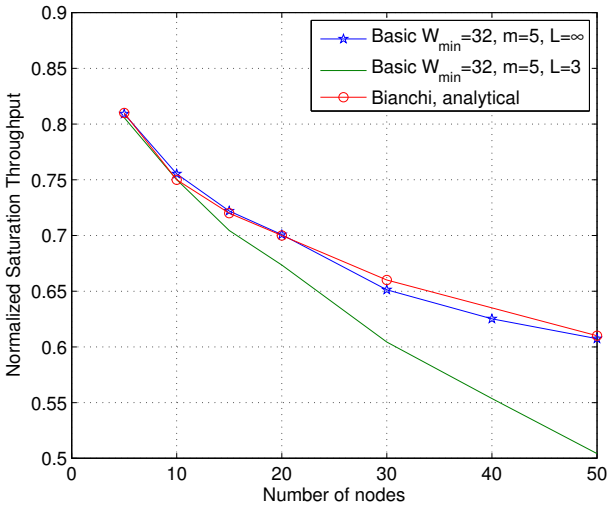

Fig. 3. Validation of OPNET simulation models.

```
Node 5 at 1.382692574998 sets DIFS after receiving ACK
Node 4 at 1.382696452150 DIFS is being set as NAV expired
Node 3 at 1.382696475336 DIFS is being set as NAV expired
Node 2 at 1.382696551985 DIFS is being set as NAV expired
Node 6 at 1.382696570325 DIFS is being set as NAV expired
```

Fig. 4. Timings for the occurrence of DIFS event in a five node network.

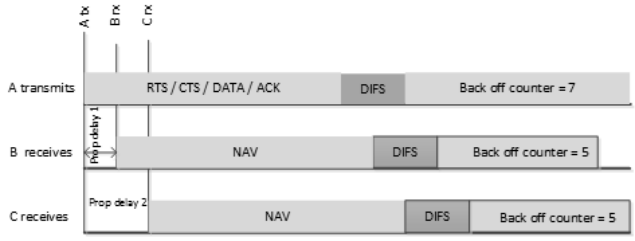

Fig. 5. Drift in DIFS due to propagation delay.

the channel among other variables affecting the models. Figure 4 shows the timings for the occurrence of DIFS event in a five node network as captured during an OPNET simulation run. In this simulation, once a data packet is received all nodes synchronize their clocks and then set the network allocation vector (NAV) variable. In this particular scenario Node 5 transmits and after receiving an ACK sets its DIFS timer. Nodes 2, 3, 4 and 6 wait for the NAV time to expiry before setting their DIFS timer. The drift in the timings at each node due to propagation delay can be clearly noticed (processing delays at nodes were maintained equal to zero). This same phenomena is also mentioned in [8] and [9] when real wireless nodes were used in an experiment.

To illustrate the impact of propagation delays Figure 5 shows the timeline of events at 3 nodes A, B and C which are sharing the media using IEEE 802.11 DCF. First, node A transmits an RTS message. Nodes B and C depending on their relative positions receive the RTS message after a time

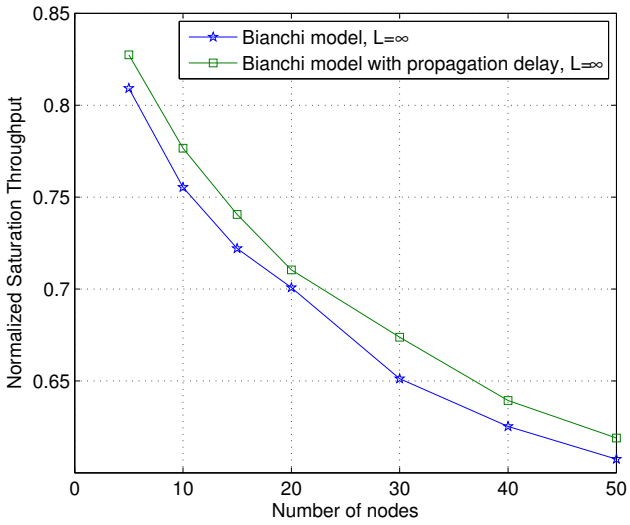

Fig. 6. Propagation delay impact on normalized saturation throughput.

"prop delay 1" and "prop delay 2", respectively. For clarity of presentation these delays are shown exaggerated but typical values are in sub-microseconds (see Figure 4). As can be seen, nodes B and C calculate their respective NAV values, which end at slightly different times. Then, the variability in propagation delay results in nodes B and C starting and ending their DIFS timers with a slight time shift. In this case, in Figure 5 we show that nodes B and C pick the same random number for their back-off counter, namely the number 5, after the DIFS timer ends. However, node B completes its back-off count down before node C and thus gets to transmit before. If the received signal is perceived at node C before its countdown ends, node C will enter a counter freeze mode as it senses carrier. Thus, transmissions from nodes B and C, which could have resulted in a collision, now result in two consecutive successes, which in turn translates into an improvement in the performance results for the IEEE 802.11 DCF protocol. This performance improvement is captured in Figure 6, which compares the normalized saturation throughput simulation results from a MAC setup as consider in [1] and from the same setup but incorporating detailed propagation delay differences between the nodes. Also, Table I details the average number of collisions in both cases. It can be seen that on average only a few collisions are avoided to become two consecutive successes, making the impact on the overall throughput not very significant.

The results presented so far assumed in the setup that the clock at every receiving node were synchronized with the reception of a signal. Figure 7 shows the normalized saturation throughput results without enabling in the OPNET simulations the synchronization when receiving a signal. This change of assumption in the setup resulted in that more transmissions that previously would have fell in the same back-off counter slot and resulted in a collision, now would not fall on the same slot and result in sequential successes instead of collisions. As the results in the Figure show, there is a very

Number of nodes	Bianchi Model		Bianchi Model with Prop. Delay	
	Average Number Coll.	Average Number Succ.	Average Number Coll.	Average Number Succ.
50	1007	1231.8	714.6	1511
40	880.6	1352.4	661.8	1561.8
30	750.8	1476.4	573.6	1645.8
20	573	1645.2	478.4	1735.2
15	490.79	1720.6	399.8	1808.6
10	366.6	1834.4	305	1895
5	210.4	1967.6	202.25	2020

TABLE I
IMPACT OF PROPAGATION DELAY ON SUCCESSES AND COLLISIONS

Number of nodes	Unsynch. Clocks		Bianchi Model (Synch. clocks)	
	Average Number Coll.	Average Number Succ.	Average Number Coll.	Average Number Succ.
50	98.4	2125.6	742.8	1479.25
40	69.2	2153.4	696.6	1527.2
30	43.8	2176.2	629.2	1590.6
20	28	2189	500.4	1711.6
15	18.6	2194.4	443.6	1763.6
10	11.2	2195.6	355.8	1843.6
5	4	2183.6	202.25	1975.25

TABLE II
IMPACT OF CLOCK SYNCHRONIZATION ON SUCCESSES AND COLLISIONS

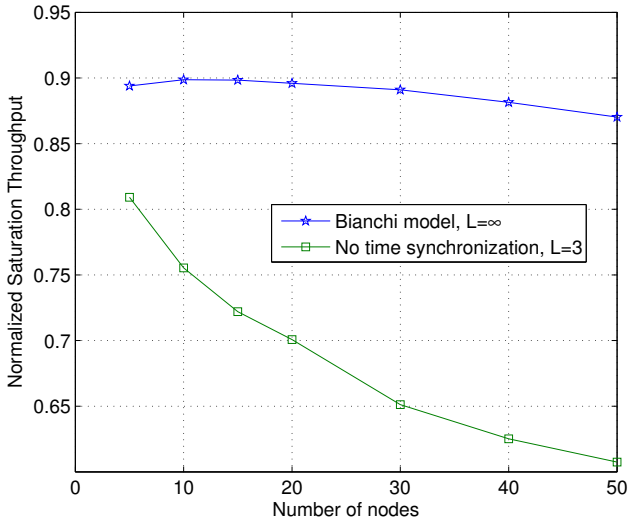

Fig. 7. Performance impact resulting from disabling synchronization.

positive impact on performance that is attributable to the lack of clock synchronization. Without clock synchronization, the normalized saturation throughput is significantly higher even as the number of contending nodes increased. Table II presents the average number of successes and collisions in each of the models with and without clock synchronization. The values were averaged over five seeds.

IV. IMPROVED CSMA/CA MEDIUM ACCESS THROUGH ADDITION OF MICRO-SLOTS

As seen in Figure 7, lack of clock synchronization improves the performance in terms of normalized saturation throughput by almost 50% in the case of 50 nodes. While this improvement in normalized saturated throughput is gradually reduced as the number of contending nodes is decreased, lack of synchronization improves the normalized saturation throughput performance for any number of nodes. However, unsynchronized clocks cannot be implemented in practice because they lead to bit detection errors and misinterpretation of the arriving bit stream. This is a major setback to the otherwise significantly positive impact observed under lack of synchronization. In this article we propose a solution to this issue that reduces the number of collisions by effectively exaggerating the effect of differences in the propagation delay. The solution consists on artificially introducing jitter in the slot time duration when a node counts down to zero, just before switching from receive to transmit mode.

For the proposed novel medium access mechanism it is still important to adhere to the slot times specified in the standards [10]. Hence, we make the following modification to the contention mechanism: at the end of the standard slot time (lasting 50 microseconds for the frequency hoping spread spectrum PHY mode), a number of extra micro slots, named in this way because they last for a much short time than the standard slot time, are introduced. The standards specify that a node can freeze its countdown 16μs before the 50μs slot time ends. Hence we set the maximum jitter to not exceed beyond 30μs, i.e. less than 50-16 μs). These timings are consistent with the timing requirements for both the PHY and MAC, and their interaction, set by the standard (e.g. Figure 17-8 Receive PLCP- in [10]). Consequently, three scenarios were considered:

- Four micro slots, each lasting 8μs,
- Six micro slots, each lasting 5μs,
- Nine micro slots, each lasting 4μs.

When operating with the proposed medium access mechanism, once a node reaches the end of the back-off countdown, it picks a number between zero and the number of existing micro slots following a uniformly distributed random choice and counts down to zero from this number, with each decrement lasting the duration of a micro slot. Once the count down has reached zero the node proceeds with transmission.

The impact of jitter in the slot times is captured in Figure 8. For comparison Bianchi's result from [1] with $L = \infty$ is included. The results in Figure 8 also show the normalized saturation throughput obtained with the proposed technique. For the case when the scheme uses 4 micro-slots, the figure shows results with $L = \infty$ and $L = 3$. It can be seen

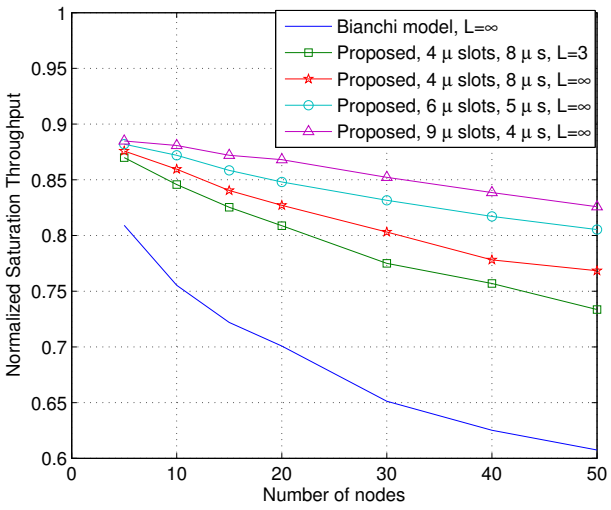

Fig. 8. Performance of proposed medium access control scheme.

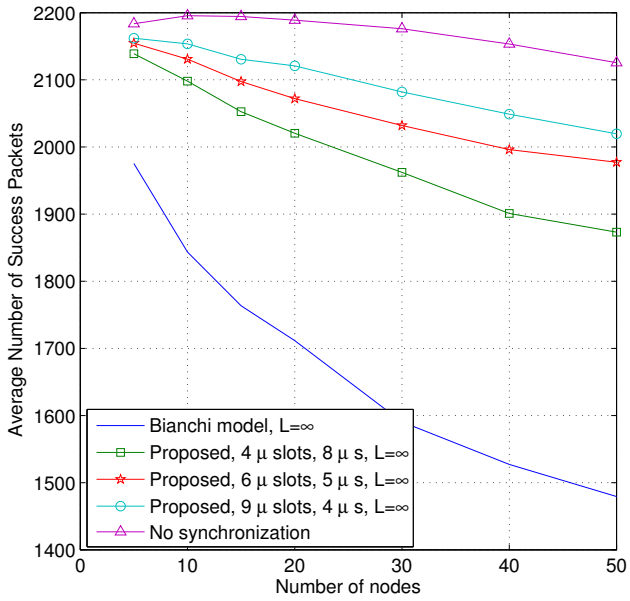

Fig. 9. Average number of successful packet transmission attempts.

that the proposed scheme achieves a clear improvement in the normalized saturation throughput. For example, when the number of micro-slots is equal to four, the improvements in normalized saturated throughput with the new technique ranges from 14% for 10 nodes up to 26% for 50 nodes (for fair comparison, these results correspond to the case when $L = \infty$). This improvement increases with the number of micro-slots to 17% for 10 nodes and 36% for 50 nodes when the number of micro-slots is nine.

Figure 9 shows the number of successful packet transmission attempts as a function of the number of nodes and averaged over the different seeds of the simulation run. While Bianchi's model from [1] exhibits a drop by 50% in the average number of successfully delivered packets, the model without enforcing clock synchronization shows improvements in the average number of successfully delivered packets ranging from a 11% improvement for the scenario with five nodes to approximately a 44% increase for the scenario with fifty nodes. The figure validates that the proposed medium access control mechanism performs well in emulating the performance improvements that could be obtained in an unrealizable scheme without clock synchronization by also showing improvements in the average number of successfully delivered packets. Indeed, for the case with the smallest number of micro-slots (four) the average number of successful packet transmission attempts is increased from 8% when there are five nodes to 27% when there are fifty nodes. The improvement in average number of successfully delivered packets increases with the number of micro-slots. As shown in Figure 9, when the number of micro-slots is nine, the average number of successful packet transmission attempts is increased from 9% when there are five nodes to 37% when there are fifty nodes.

V. Analytical Model for CSMA/CA Medium Access with Micro-slots

In this section we revisit Bianchi's model for IEEE 802.11 DCF from [1], now with the addition of time jitter. As a practical matter, and as previously discussed, multiple nodes in a one-hop network may behave asynchronously even though the IEEE 802.11 DCF medium access protocol tries to prevent it. Each pair of nodes can experience a different propagation delay and, even if synchronized, all clocks will run at a slightly different rate. The result is that when two or three nodes (in the back-off process) count down to zero "at the same time", there may be enough of a time differential that the first node to send is sensed by the others and a successful packet transmission goes through. Of course, within the reckoning of Bianchi's model, counts to zero are simultaneous and multiple senders always results in a collision.

To address this discrepancy, we modify Bianchi's model by requiring that each contending node (i.e. one having just counted to zero) must enter a micro-contention window, μCW, containing some number ν of micro-slots. The micro-slot times are very short, but long enough to allow a sender in one micro-slot to be sensed by a sender in the next slot. The only purpose of the μCW is to serialize multiple sending nodes in an attempt to avoid collisions. Of course, there may still be some collisions as multiple nodes may populate the same micro-slot.

Because these micro-slots are supposed to reflect clock differences among multiple nodes, we will not assume that each micro-slot has the same probability of being occupied. This is handled by letting the set of probabilities $\{\phi_1, \phi_2, \ldots, \phi_\nu\}$ specify the likelihood of a sending node falling into each micro-slot. A significant difference between a μCW and a regular contention window, CW, is that the population distribution of the μCW never comes to equilibrium. Within each regular slot, the μCW is populated and then fully depleted. At each back-off counter decrement, the μCW is always empty. However, because the μCW changes the probabilities of success

and collision, the Bianchi values for the probabilities τ and p, which retain their original meaning as introduced in (1) and (2), must also change their value. Thus, the states of the Markov chain introduced in Bianchi's model stay the same but some of the transition probabilities must change.

Considering the possible changes to τ and p, (1) still holds in the modified model, but equation (2) changes. Looking at it from the viewpoint of a tagged node, τ is the probability that the node will try to send in any given slot. Given that the tagged node is trying to send, the probability of it falling into the i^{th} micro-slot equals ϕ_i. Thus, the probability of the tagged node falling into the i^{th} micro-slot in any given time slot is $\tau\phi_i$. Now consider the $n-1$ remaining nodes in the network. The probability that each one will also fall into the i^{th} micro-slot is $\tau\phi_i$ and so the probability of each one NOT falling into the i^{th} micro-slot is $1-\tau\phi_i$. Then, the probability that *none* of the remaining nodes falls into the i^{th} micro-slot is $(1-\tau\phi_i)^{n-1}$. Finally, the probability that another node collides with the tagged node in the i^{th} micro-slot is $1-(1-\tau\phi_i)^{n-1}$.

Given that the tagged node is trying to send, we find the unconditioned probability that the tagged node experiences a collision (p), by computing the collision probabilities from each micro-slot and take a weighted average according to the micro-slot population probabilities. So, the probability of a collision for the tagged node now is

$$p = \sum_{i=1}^{\nu} \phi_i \left[1-(1-\tau\phi_i)^{n-1}\right]. \quad (3)$$

As before, solving the simultaneous system, (1) and (3), will produce values for τ and p.

We now turn our attention to S, the normalized saturation throughput. The initial expression from [1],

$$S = \frac{E[\text{payload information transmitted in a slot time}]}{E[\text{length of a slot time}]}, \quad (4)$$

is still applicable but from this point on some changes are needed in the derivation of S in [1]. This is because Bianchi's model in [1] allows only one of three possible events in any slot:

1) IDLE; no transmissions, **or**
2) a single SUCCESS: a case of a successfully transmitted packet, **or**
3) a single COLLISION: one case of multiple concurrent transmissions.

With the introduction of a μCW, we can possibly have, within any slot the following three possible events:

1) IDLE; no transmissions, **or**
2) one or more cases of SUCCESS, **and/or**
3) one or more cases of COLLISION.

When there could only be zero or one success, there was no difference between the probability of a single success and the expected number of successes. Now these values are different because of the possibility of multiple successes. Next, we calculate the probability of the three possible events within any slot. As we have already seen, in any given slot, the probability that a given node will fall into the i^{th} micro-slot is $\tau\phi_i$ and the probability that the given node will NOT fall into the i^{th} micro-slot is equal to $1-\tau\phi_i$. Therefore,

1) the probability that the i^{th} micro-slot has zero nodes is $(1-\tau\phi_i)^n$,
2) the probability that the i^{th} micro-slot has one node is $n\tau\phi_i(1-\tau\phi_i)^{n-1}$,
3) the probability that the i^{th} micro-slot has two or more nodes is $1-(1-\tau\phi_i)^n - n\tau\phi_i(1-\tau\phi_i)^{n-1}$

Because micro-slots are similar to the original slots in [1] in that exactly one of these three possible events happens, the probabilities for the second and third event are also the expected values of the number of successes and the number of collisions, respectively, within the i^{th} micro-slot. Next, to find the unconditioned expected values for successes (denoted as $E[\#\text{S}]$) and collisions (denoted as $E[\#\text{C}]$, we have to sum across micro-slots. Therefore, for any single slot, we get,

$$E[\#\text{S}] = \sum_{i=1}^{\nu} n\tau\phi_i(1-\tau\phi_i)^{n-1}, \quad (5)$$

$$E[\#\text{C}] = \sum_{i=1}^{\nu} \left[1-(1-\tau\phi_i)^n - n\tau\phi_i(1-\tau\phi_i)^{n-1}\right] \quad (6)$$

As before, because the slot is either empty or it is not, the expected number of idle events in a slot (denoted as $E[\#\text{I}]$) is equal to the probability of the slot being idle. Thus,

$$E[\#\text{I}] = (1-\tau)^n. \quad (7)$$

Now, letting T_p denote the packet transmission time, and using (4) we can write the normalized saturation throughput as

$$S = \frac{E[\#\text{S}]T_p}{E[\#\text{I}]\sigma + E[\#\text{S}]T_s + E[\#\text{C}]T_c}, \quad (8)$$

where σ is the duration of an empty slot time, T_s is the average time the channel is sensed busy because of a successful transmission and T_c is the average time the channel is sensed busy by each station during a collision.

We conducted further evaluations of the proposed medium access control scheme based on the introduction of micro-slots. Figure 10 shows results obtained from both OPNET simulations and the analytical model presented in this section. It can be seen that the improvements achieved in the simulations are also reflected in the results obtained from the analytical model presented above. The results show improvements in normalized saturated throughput with the new technique from 14% for 10 nodes up to 26% for 50 nodes. The normalized saturation throughput obtained from the analytical model is lower than the simulation result because the latter also accounts for the effect of the varying propagation delays. As previously discussed, different propagation delays have the effect of increasing the probability of successful transmission attempt. This improvement increases with number of nodes, because when there are more nodes the spacing between more likely distant nodes introduces more distinct propagation delay effects.

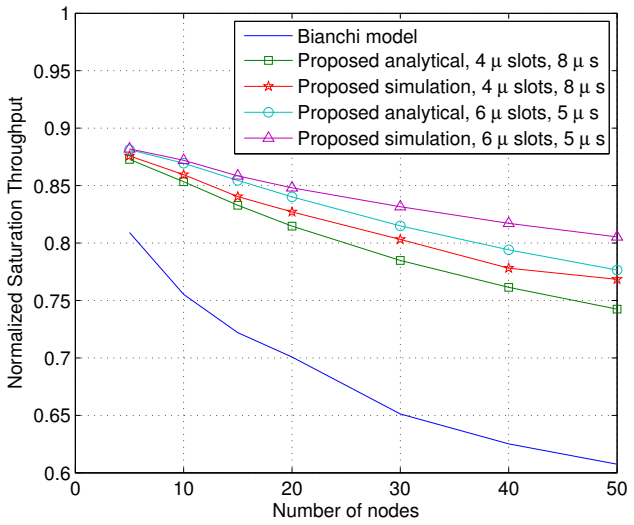

Fig. 10. Impact of jitter in slot times both from simulations and analytical model ($L = \infty$).

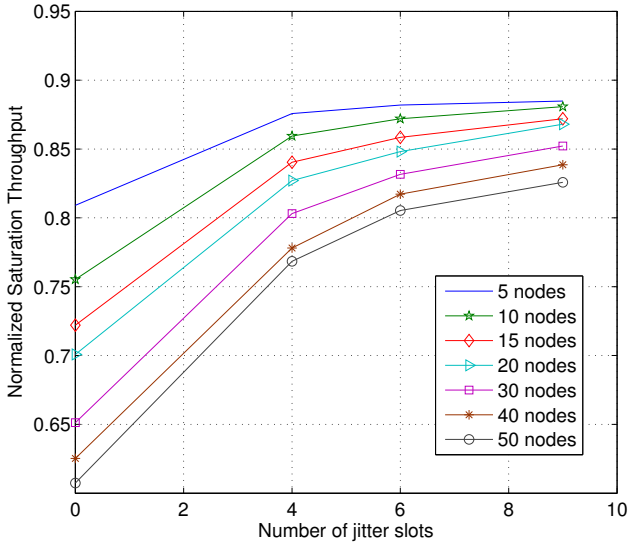

Fig. 11. Normalized saturation throughput as a function of number of micro-slots ($L = \infty$).

Finally, Figure 11 depicts the change in normalized saturation throughput achieved by increasing the number of micro-slots when jitter is introduce in the slot-time of 50μs and with different number of stations as parameter. In the case of five nodes the change of normalized saturation throughput is less than the cases with larger number of stations. For example, for the case of 50 nodes, increasing the number of slots from 0 to 9 increased throughput from 0.61 to 0.82

VI. Conclusion

In this paper we have studied the effects of different propagation delays and lack of clock synchronization on the performance of the IEEE 802.11 DCF medium access control protocol. Based on a detailed OPNET simulation model, we observed that different propagation delays and lack of clock synchronization results in an increase in normalized saturated throughput. While the increase in throughput is modest when resulting from different propagation delays, it is significant when the nodes are not synchronized with the reception of a signal. Nevertheless, this performance improvements cannot be directly exploited because unsynchronized clocks can lead to bit detection errors and misinterpretation of the arriving bit stream.

Consequently, the second major novel contribution in this paper leverages the lessons learned from the performance study and introduces a new CSMA/CA medium access technique. In the proposed technique, a random short delay is introduced at the end of the back-off period. This short delay, akin to jitter, emulates the mechanism that results in increased saturated throughput with different propagation delays and lack of clock synchronization, namely that transmissions that previously would fall in the same back-off counter slot and result in a collision, now would be serialized, resulting in sequential successes instead of collisions. Simulation results show improvements in normalized saturated throughput with the new technique from at least 14% for 10 nodes up to 26% for 50 nodes. The simulation results are also validated with our proposed analytical model.

References

[1] G. Bianci, "Performance Analysis of the IEEE 802.11 Distributed Coordination Function," *IEEE Journal on Selected Areas in Communication*, Vol. 18, no. 3, pp: 535–547, March 2000.

[2] H. Wu, Y. Peng, K. Long, S. Cheng, J. Ma, "Performance of reliable transports protocol over IEEE 802.11 wireless LAN: analysis and enhancement," *in Proceedings IEEE INFOCOM*, vol. 2, pp. 599-607, June 2002.

[3] P. Chatzimisios, A. Boucouvalas, V. Vitsas, "IEEE 802.11 packet delay-a finite retry limit analysis," *in Proceedings of IEEE Global Telecommunications Conference (GLOBECOM)*, vol. 2, pp. 950-954, Dec. 2003.

[4] C. Foh, J. Tantra, "Comments on IEEE 802.11 saturation throughput analysis with freezing of backoff counter," *IEEE Communications Letters*, vol. 9, pp. 130-132, Feb. 2005.

[5] Y. Xiao, "Performance analysis of priority schemes for IEEE 802.11 and IEEE 802.11e wireless LANs," *IEEE Transactions on Wireless Communications*, vol. 4, pp. 1506-1515, July 2005.

[6] L. Zhang, Y. Shu, O. Yang, G. Wang, "Study of medium access delay in IEEE 802.11 wireless networks," *IEICE Transactions on Communications*, vol. 89, pp. 1284-1293, April 2006.

[7] E. Felemban, E. Ekici, "Single Hop IEEE 802.11 Analysis Revisited: Accurate Modeling of Channel Access Delay and Throughput for Saturated and Unsaturated Traffic Cases," *IEEE Transactions on Wireless Communications*, Vol. 10, no. 10, pp: 3256–3266, October 2011.

[8] D. Malone, I. Dangerfield, D. Leith, "Verification of Common 802.11 MAC Model Assumptions," *Proceedings of the 8th International Conference on Passive and Active Network Measurement (PAM'07)*, pp. 63–72, 2007.

[9] Huang, K.D.; Duffy, K.R.; Malone, D.; Leith, D.J.; "Investigating the Validity of IEEE 802.11 MAC Modeling Hypotheses," *IEEE 19th International Symposium on Personal, Indoor and Mobile Radio Communications (PIMRC)*, pp.1-6, 15-18 Sept. 2008.

[10] IEEE 802.11 Working Group, "Wireless LAN Medium Access Control (MAC) and Physical Layer (PHY) Specifications," March 2012.